Atmospheric
Chemistry
and Physics

Supplement of

Water vapour adjustments and responses differ between climate drivers

Øivind Hodnebrog et al.

Correspondence to: Øivind Hodnebrog (oivind.hodnebrog@cicero.oslo.no)

Contents of this file

Introduction

This file includes supporting Text, Figures and Tables as referenced from the main manuscript.

Text S1.

The ECHAM-HAM model was run at T63 (approx. 1.85 x 1.85 degrees) horizontal resolution and 31 vertical levels (up to 10 hPa) using the latest version ECHAM6.3-HAM2.3-M7 with online aerosol processing. The previous version of ECHAM-HAM is described in Zhang et al. (2012). The baseline aerosol emissions in ECHAM-HAM were ACCMIP year 2000 (Lamarque et al., 2010), and for the perturbed BC runs all BC sources (agricultural waste burning, aircraft, domestic, energy, forest and grass fires, industry, shipping, energy and waste) were scaled. For the coupled ECHAM-HAM runs a slab ocean was used (apart from NCAR-CESM1-CAM4, the other models used a full dynamical ocean). ECHAM-HAM is essentially the same model as MPI-ESM except for the aerosol and stratiform cloud scheme, and have only run the BCx10 perturbation experiment (the other models did all experiments except that MPI-ESM did not perform the aerosol perturbation experiments).
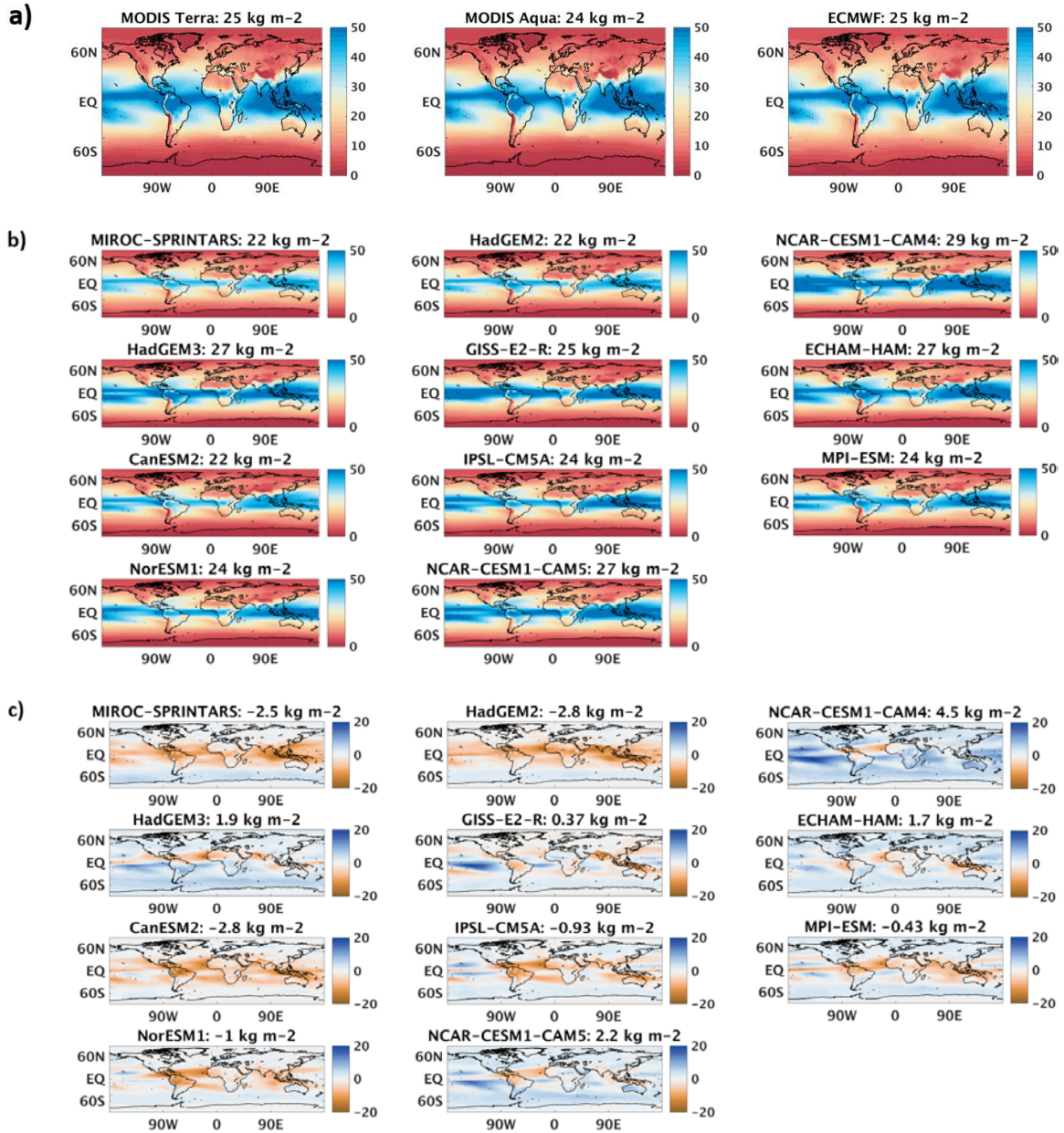
Figure S1. Integrated water vapour (kg m^{-2}) in a) observations/reanalysis (see Section 2 in main manuscript), b) in the PDRMIP coupled base model simulations, and c) as difference between each model and the mean of the three observations/reanalysis datasets. The HadGEM2 baseline is representative of pre-industrial conditions and therefore likely an underestimate compared to the present-day integrated water vapour.
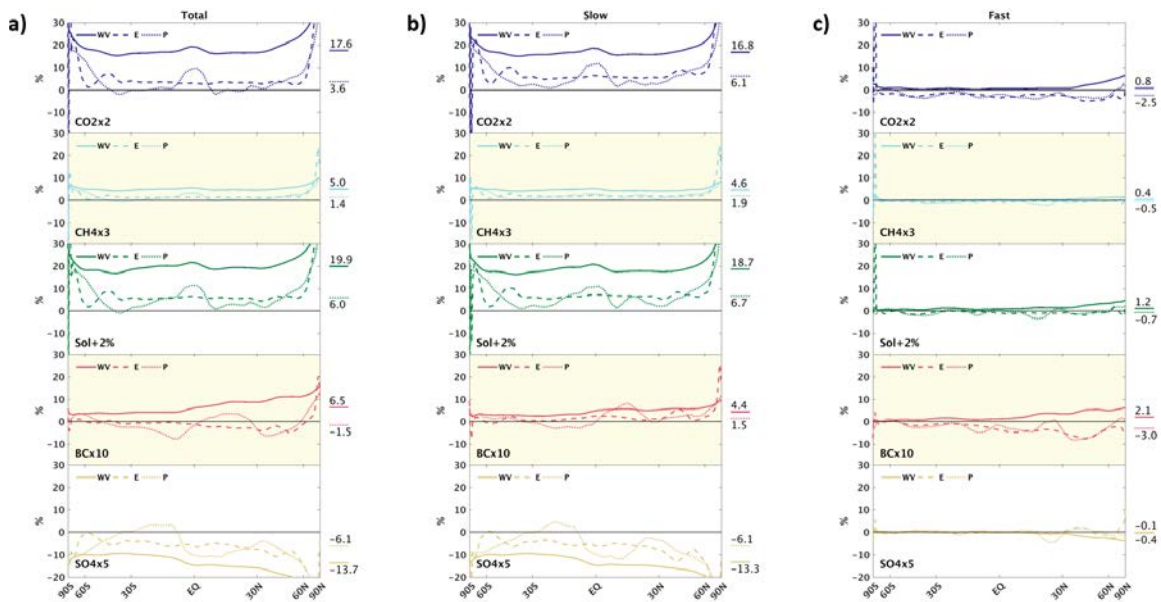
Figure S2. Relative changes in integrated water vapour (WV), evaporation (E), and precipitation (P) for five different drivers, split into a) total, b) slow, and c) fast responses. Global mean values are given to the right of each plot (note that evaporation and precipitation are equal in the global mean). In some cases, relative evaporation changes are large at very high latitudes and exceed the scale shown.
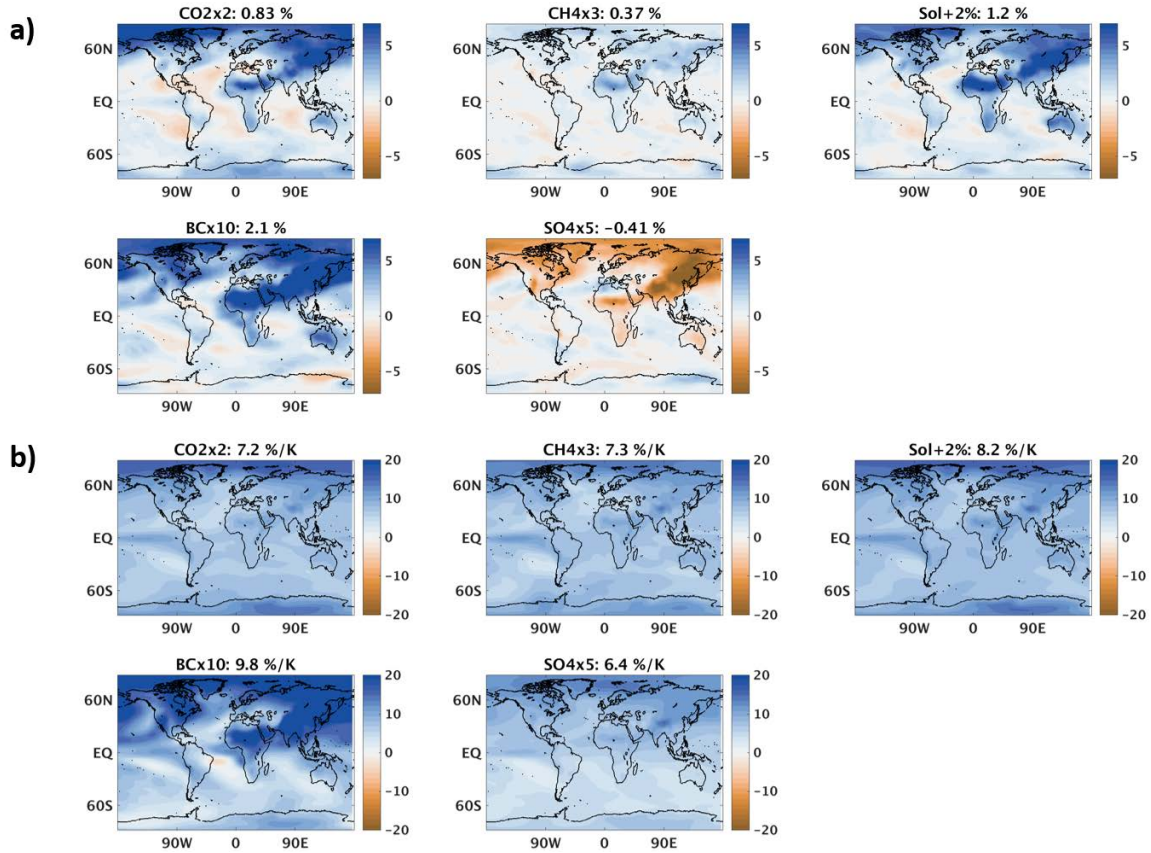
Figure S3. Maps of model mean relative change in integrated water vapour for each driver in the PDRMIP a) fixed SST and b) coupled simulations. The coupled simulation results are normalized by the global mean surface temperature change for each driver.
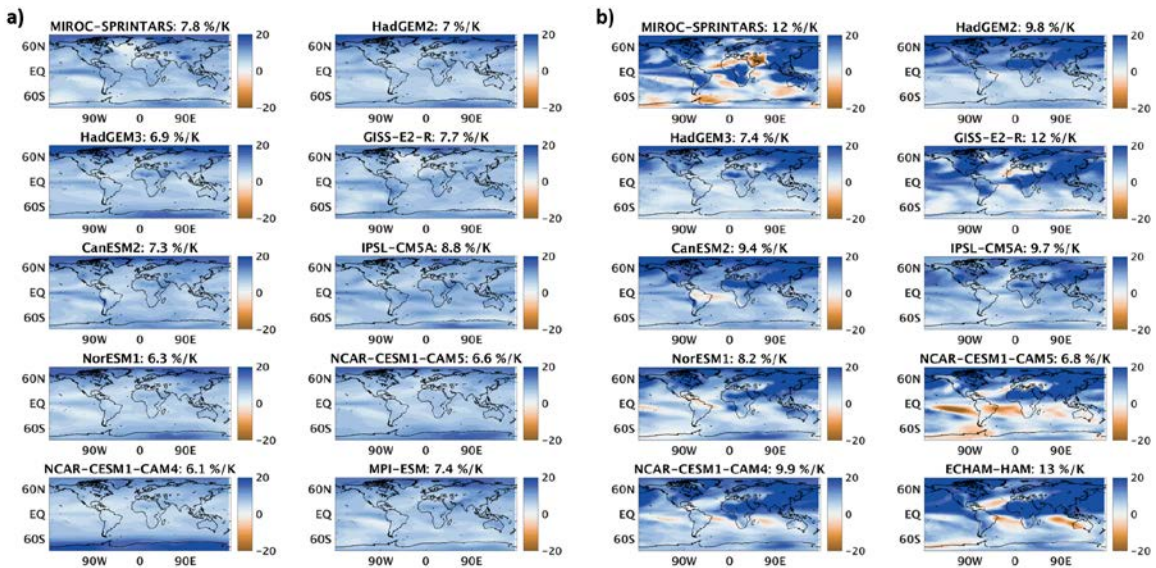

Figure S4. Maps of relative change in integrated water vapour per degree surface temperature change (%/K) for a) CO2x2 and b) BCx10 in each of the PDRMIP coupled models.
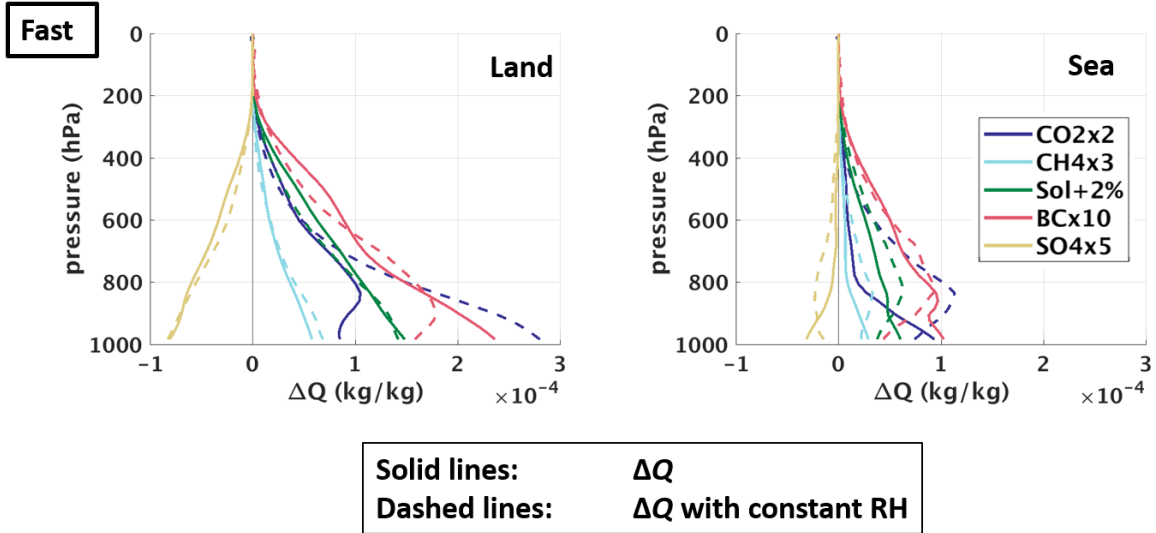
5

Figure S5. Fast changes in specific humidity (ΔQ) over land (left) and sea (right). Dashed lines show expected specific humidity changes from the Clausius-Clapeyron relation assuming constant relative humidity.
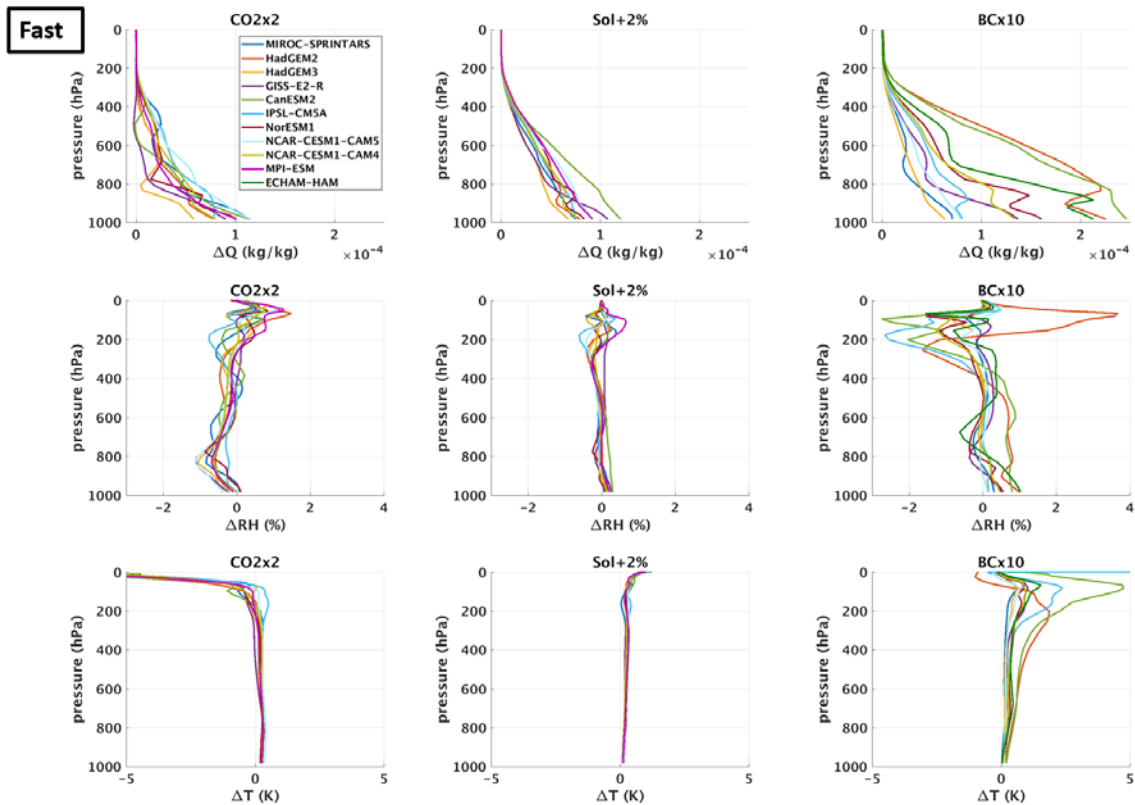

Figure S6. Vertical profiles of changes in specific humidity (top), relative humidity (middle) and temperature (bottom) for CO2x2 (left), Sol+2% (middle), and BCx10 (right) in the PDRMIP fixed SST simulations.
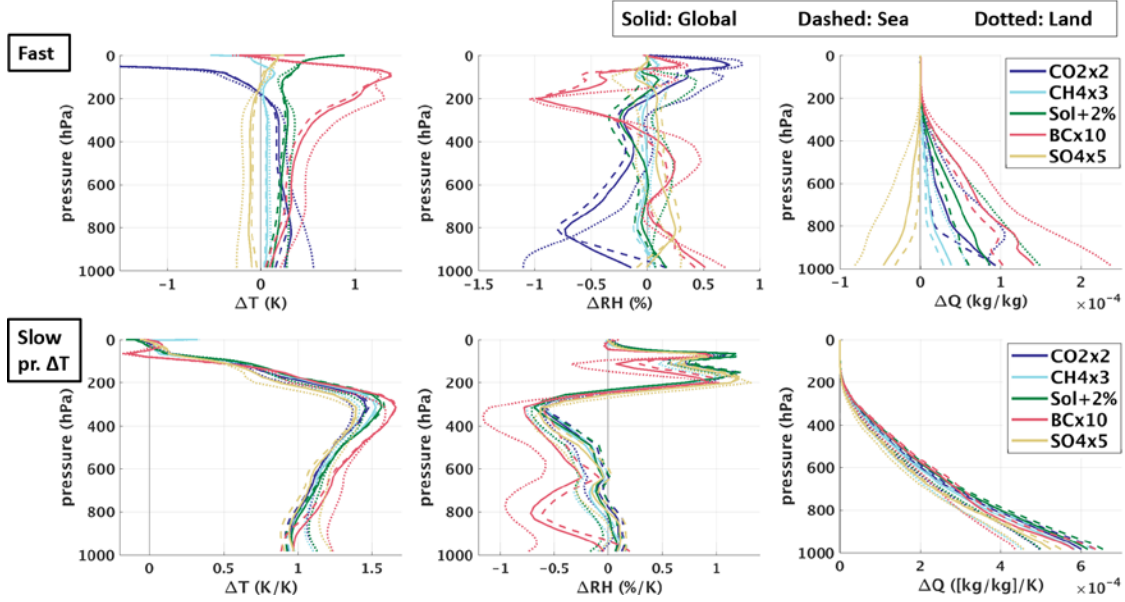
Figure S7. Model mean vertical profiles, separated into global (solid lines), sea only (dashed) and land only (dotted), of changes in temperature (ΔT; left), relative humidity (ΔRH; middle), and specific humidity (ΔQ; right). The top row shows fast responses and the bottom row shows slow responses divided by the global mean surface temperature change induced by each driver.

	Historical RF[a] (W m^{-2})	PDRMIP experiment	PDRMIP RF (W m^{-2})	PDRMIP fast Δτ (days)	Historical fast Δτ (days)
CO_2	1.2502	CO2x2	3.70	0.282	0.0956
CH_4	0.4126	CH4x3	1.17	0.0725	0.0272
N_2O	0.1271	CH4x3	1.17	0.0725	0.0084
Halocarbons	0.3316	CH4x3	1.17	0.0725	0.0219
BC[b]		BCx10	1.17	0.429	0.0429
Scattering aerosols	-1.5[c]	SO4x5	-3.53	-0.0275	-0.0087

[a]Values are from IPCC AR5 (Myhre et al., 2013) for year 1996 (middle of 1986-2005 period in Fig. 1) minus 1860 (middle of 1850-1869 period in Fig. 1).
[b]10% of the RF in BCx10 experiment has been assumed for BC.
[c]Historical RF of scattering aerosols has been derived as the difference between total aerosols (-0.9 W m^{-2} (Myhre et al., 2013)) and BC (0.6 W m^{-2} (Myhre et al., 2013)).

Table S1. Historical fast water vapour lifetime change (Δτ) calculated for important climate drivers based on combining the historical top of the atmosphere radiative forcing (RF) with results from PDRMIP experiments. The calculations were done separately for each PDRMIP model and the table shows the multi-model mean of these results. The historical lifetime change for ozone and surface albedo has not been calculated due to lack of data.

References

Lamarque, J. F., Bond, T. C., Eyring, V., Granier, C., Heil, A., Klimont, Z., Lee, D., Liousse, C., Mieville, A., Owen, B., Schultz, M. G., Shindell, D., Smith, S. J., Stehfest, E., Van Aardenne, J., Cooper, O. R., Kainuma, M., Mahowald, N., McConnell, J. R., Naik, V., Riahi, K., and van Vuuren, D. P.: Historical (1850–2000) gridded anthropogenic and biomass burning emissions of reactive gases and aerosols: methodology and application, Atmos. Chem. Phys., 10, 15, 7017-7039, 10.5194/acp-10-7017-2010, 2010.

Myhre, G., Shindell, D., Bréon, F.-M., Collins, W., Fuglestvedt, J., Huang, J., Koch, D., Lamarque, J.-F., Lee, D., Mendoza, B., Nakajima, T., Robock, A., Stephens, G., Takemura, T., and Zhang, H.: Anthropogenic and Natural Radiative Forcing, in: Climate Change 2013: The Physical Science Basis. Contribution of Working Group I to the Fifth Assessment Report of the Intergovernmental Panel on Climate Change, edited by: Stocker, T. F., Qin, D., Plattner, G.-K., Tignor, M., Allen, S. K., Boschung, J., Nauels, A., Xia, Y., Bex, V., and Midgley, P. M., Cambridge University Press, Cambridge, United Kingdom and New York, NY, USA, 659–740, 2013.

Zhang, K., O'Donnell, D., Kazil, J., Stier, P., Kinne, S., Lohmann, U., Ferrachat, S., Croft, B., Quaas, J., Wan, H., Rast, S., and Feichter, J.: The global aerosol-climate model ECHAM-HAM, version 2: sensitivity to improvements in process representations, Atmospheric Chemistry and Physics, 12, 19, 8911-8949, 10.5194/acp-12-8911-2012, 2012.